Soil Use and Management

Soil Use and Management, December 2009, **25,** 354–361 doi: 10.1111/j.1475-2743.2009.00218.x

Estimation and analysis of soil hydraulic properties through infiltration experiments: comparison of BEST and DL fitting methods

X. Xu, G. Kiely & C. Lewis

Department of Civil and Environmental Engineering, Centre for Hydrology, Micrometeorology and Climate Change, University College Cork, Cork, Ireland

Abstract

The BEST method (Beerkan estimation of soil transfer parameters through infiltration experiments) appears promising and easy to estimate not only saturated hydraulic conductivity but also water retention and hydraulic characteristics. However, few tests have been conducted to test the methodology. This study involved field BEST infiltration experiments for three layers (surface, 15 and 30 cm) for each of three soils with different soil textures under grassland. By comparing BEST with DL (differentiated linearization method), we found that the DL method did not produce a good estimate of the soil hydraulic properties and neither did it identify the transient flow state. The BEST method resulted in reasonable results and is therefore promising. However, with BEST we encountered some anomalies when calculating hydraulic properties in some cases with too few data points under the transient flow state. We show that the application of BEST field experiments requires a wide range of soil water content from initial to saturated states so as to include sufficient transient flow. The soil hydraulic properties determined using the BEST method showed contrasting characteristics between different soil textures with higher saturated hydraulic conductivity under coarse texture and lower values under loam textures, especially with highly compacted soils. Vertical variation in soil hydraulic properties was significant, and the surface layer had a lower saturated hydraulic conductivity partly caused by compaction (high bulk density) or by remnants of grass plants. Further research on the effects of compaction and grass plants on soil hydraulic properties is needed.

Keywords: Soil hydraulic properties, Beerkan method, differentiated linearization method

Introduction

Soil hydraulic properties are important for modelling hydrological processes and related contamination transport. Some soil hydraulic properties can be obtained in the laboratory using undisturbed soil samples, and some can be obtained in the field using different measurement techniques. Among these methods, the Beerkan method proposed by Braud *et al.* (2005) and its enhanced version, the BEST method (Beerkan estimation of soil transfer parameters through infiltration experiments) by Lassabatère *et al.* (2006), appear to be promising, easy, robust and inexpensive. BEST involves a simple field infiltration experiment using a ring at the soil surface (and at different depths) to estimate not only the saturated hydraulic conductivity but also water retention and hydraulic characteristics. To make the BEST method more practical in the field at a much lower cost, Minasny & McBratney (2007) developed an alternative way of estimating the van Genuchten (1980) water retention shape parameter *n* from a soil's sand and clay content instead of from the particle size distribution. Another important issue is to estimate sorptivity and saturated hydraulic conductivity through fitting infiltration data with some specific algorithms. Vandervaere *et al.* (2000a,b) proposed linearizing the experimental data by differentiating cumulative infiltration with respect to the square root of time which allows a visual check and linear fitting (differentiated linearization, DL method). Minasny & McBratney (2000) and Jacques *et al.* (2002) identified some problems with this method but did not carry out further analysis. In the study by Lassabatère *et al.* (2006), no anomalies were encountered when modelling cumulative infiltration with BEST, and it appeared a promising and easy

Correspondence: X. Xu. E-mail: xuxianliww@gmail.com; xuxianli@sohu.com
Received December 2008; accepted after revision March 2009

method. However, few studies have been conducted to test this.

Soils with contrasting textures have different soil hydraulic behaviours (Clapp & Hornberger, 1978). Soil texture and structure vary greatly in space and result in soil hydraulic parameters also varying widely in space. The variation in these parameters can lead to further uncertainty in estimating run-off generation in spatially distributed hydrological modelling (Herbst *et al*., 2006). Jhorar *et al*. (2004) pointed out that vertical variation in soil hydraulic parameters should not be neglected for successful application of hydrological models.

This study selected three soils under grassland with widely contrasting textures for Beerkan infiltration experiments using samples from different layers of each soil with the aims to: (1) test and compare BEST and DL fitting methods and (2) analyse the infiltration processes and hydraulic behaviour of differently textured soils and their vertical variation.

Materials and methods

BEST and DL fitting method

The BEST infiltration method is based on the van Genuchten relationship for the water retention curve (equation 1a) with the Burdine condition (equation 1b) and the Brooks and Corey relationship (equation 2) for hydraulic conductivity (Burdine, 1953; Brooks & Corey, 1964; van Genuchten, 1980):

$$\frac{\theta-\theta_r}{\theta_s-\theta_r}=\left[1+\left(\frac{h}{h_g}\right)^n\right]^{-m} \tag{1a}$$

$$m=1-\frac{2}{n} \tag{1b}$$

$$\frac{K(\theta)}{K_s}=\left(\frac{\theta-\theta_r}{\theta_s-\theta_r}\right)^{\eta} \tag{2a}$$

$$\eta=\frac{2}{\lambda}+2+p, \quad \text{with } \lambda=mn \tag{2b}$$

where n, m and η are shape parameters and h_g, θ_s, θ_r and K_s are scale parameters. Usually, θ_r is very low and thus considered to be zero. p is a tortuosity parameter that depends on the chosen capillary model, and a value of 1 is used here following Burdine's condition (Burdine 1953; Braud *et al*., 2005). n is calculated as proposed by Minasny & McBratney (2007):

$$n=2.18+0.11[48.087-44.954S(x_1)-1.023S(x_2)-3.896S(x_3)] \tag{3a}$$

where

$$x_1=24.547-0.238\times\text{sand}-0.082\times\text{clay} \tag{3b}$$

$$x_2=-3.569+0.081\times\text{sand} \tag{3c}$$

$$x_3=0.694-0.024\times\text{sand}+0.048\times\text{clay} \tag{3d}$$

where 'sand' and 'clay' refer to sand and clay content (%, w/w) and

$$S(x_i)=\frac{1}{1+\exp(-x_i)}. \tag{3e}$$

BEST estimates K_s and h_g parameters from infiltration experiments by using a specific algorithm whose main characteristics are briefly described below, and the details can be found in the study by Lassabatère *et al*. (2006). BEST is referred to BEST/I or BEST/q according to the choice of time series: I (cumulative infiltration depth) or q (infiltration rate). This study used only the BEST/I method as Lassabatère *et al*. (2006) showed that BEST/I performed better than BEST/q. Consider an infiltration experiment with zero pressure on an r_d internal radius circular surface above a uniform soil with a uniform initial water content; the three-dimensional cumulative infiltration and infiltration rate can be approached by the explicit transient two-term equation (equation 4a) and steady-state expansion (equation 4b).

$$I(t)=S\sqrt{t}+(AS^2+BK_s)t \tag{4a}$$

$$q_s=AS^2+K_s \tag{4b}$$

where constants A and B can be defined for the specific case of the Brooks and Corey relation (equation 2) and taking into account initial conditions defined by (Haverkamp *et al*., 1994)

$$A=\frac{\gamma}{r_d(\theta_s-\theta_0)} \tag{5a}$$

$$B=\frac{(2-\beta)}{3}\left[1-\left(\frac{\theta_0}{\theta_s}\right)^{\eta}\right]+\left(\frac{\theta_0}{\theta_s}\right)^{\eta} \tag{5b}$$

where $\beta\approx 0.6$ and $\gamma\approx 0.75$, which apply for most soils when $\theta_0 < 0.25\theta_s$ (Haverkamp *et al*., 1994; Smettem *et al*., 1994).

BEST first estimates sorptivity by fitting the transient cumulative infiltration to the two-term equations (equation 4a). The fit is based on the replacement of hydraulic conductivity K_s by its sorptivity function S and the experimental apparent steady-state infiltration rate (q_s) through equation (4b) and the following conditions: an accurate reproduction of experimental data; a fit for S between zero and a maximum value that corresponds to a null hydraulic conductivity (capillary-driven flow) and the use of restricted data subsets to ensure the validity of equation (4a). Once sorptivity is estimated, the saturated hydraulic conductivity

is obtained through equation (4b), assuming that the steady state (apparent steady state) has been reached. The pressure head scale parameter (h_g) is then estimated from the other hydraulic parameters by equation (6)

$$S^2(\theta_0, \theta_s) = -c_p \theta_s K_s h_g \left(1 - \frac{\theta_0}{\theta_s}\right)\left[1 - \left(\frac{\theta_0}{\theta_s}\right)^{\eta}\right] \quad (6a)$$

$$c_p = \Gamma\left(1 + \frac{1}{n}\right)\left\{\frac{\Gamma\left(m\eta - \frac{1}{n}\right)}{\Gamma(m\eta)} + \frac{\Gamma\left(m\eta + m - \frac{1}{n}\right)}{\Gamma(m\eta + m)}\right\} \quad (6b)$$

where Γ is the usual Gamma function.

Vandervaere *et al*. (2000a,b) proposed the following relationships (DL method) to estimate sorptivity and saturated hydraulic conductivity by a visual check and linear fitting within limited time:

$$\frac{dI}{d\sqrt{t}} = C_1 + 2C_2\sqrt{t} \quad (7a)$$

$$S = C_1 \quad (7b)$$

$$K_s = \frac{C_2 - AC_1^2}{B} \quad (7c)$$

A and B are defined as above.

To apply the DL method, the infiltration with respect to the square root of time $\left(t^*, dI/d\sqrt{t}\right)$ from the original experimental data (t_i, I_i) was derived as follows (Vandervaere *et al*., 2000a; Lassabatère *et al*., 2006):

$$\frac{dI}{d\sqrt{t}} = \frac{I_{i+1} - I_i}{\sqrt{t_{i+1}} - \sqrt{t_i}} \quad (8a)$$

$$t^* = \left(\sqrt{t_{i+1} t_i}\right)^{0.5}. \quad (8b)$$

Field experiments

The Beerkan infiltration method is a simple three-dimensional infiltration test under a positive head, h_{sur} (the head at the soil surface) conditions, using cylinders of diameter r_d (ranging from 5 to 15 cm). The procedure is carried out in consecutive steps as follows. The surface vegetation is removed over an area slightly larger than the cylinder while the roots remain *in situ*. The test must be made on a level site. The cylinder is positioned at the soil surface and inserted to a depth no deeper than 1 cm into the topsoil to prevent lateral losses of water. A disturbed soil sample is collected (0–5 cm depth) close to but not adjacent to the cylinder, and used to determine the initial gravimetric moisture content w. Particle size (soil texture) analysis is carried out on another disturbed sample taken near the cylinder at the experimental site. A fixed volume of water (exactly 178 mL for the 14.4-cm-diameter ring corresponding to a water depth of 1.1 cm) is poured into the cylinder at time zero, and the time required for infiltration of the known volume of water is measured. As soon as the first volume has completely infiltrated, i.e. water no longer standing on the soil surface, the second known volume of water (also 178 mL) is added to the cylinder and the time needed for this to infiltrate is measured (cumulative time). The procedure is repeated until the test reaches nearly steady state (apparent steady state), indicated by the time to infiltrate each known volume (usually requires 8–15 volumes). Note that with this procedure, the surface pressure is not constant during the test (the 'falling head' test). However, Haverkamp *et al*. (1998) showed that small variations of h_{sur} do not significantly influence the results. After the experiment, an undisturbed sample of known volume (soil core) is taken close to the cylinder to obtain the soil dry bulk density, ρ_d (g/cm^3). The initial and final volumetric water content were estimated in this study using:

$$\theta_0 = w\rho_d \quad (9a)$$

$$\theta_s = 1 - \frac{\rho_d}{2.65} \quad (9b)$$

where 2.65 (g/cm^3) denotes soil particle density.

We selected three soils under grassland but with widely different soil textures (Table 1). Heavy duty plastic rings with 14.4 cm internal diameter (of wall thickness ~4 mm) with the driving edge bevelled (on the external side of the ring) were used. These tests were carried out at three depths: the surface, 15 and 30 cm, and repeated three times (replicates 1–3) at each level.

Results and discussion

Infiltration analysis, sorptivity and saturated hydraulic conductivity estimation

For the shallow brown earth (site 126) (Figure 1a,b), the infiltration process curves were similar for the second and third layers and dissimilar to the surface layer curve in replicates 1 and 2, while those curves for the surface and second layers were similar in the third replicate (Figure 1c). Infiltration approached apparent steady state earlier for the surface layer than for the other two layers and therefore the transition from the transient to the steady flow state was less clearly marked for the surface layer. For the brown podzol (site 355) (Figure 2a–c), the infiltration curve of the surface layer is lower than those of the other two layers. The infiltration features of the sand (site 879) (Figure 3a–c) are similar to the shallow brown earth and brown podzol, with the second and third layers having similar infiltration while dissimilar to the surface one. However, the infiltration for the surface layer more gradually (nonlinear) changes from a high to a low rate of infiltration and its apparent steady-state infiltration rate is lower than the other two layers (Figure 3a–c and Table 2).

Table 1 Soil conditions for three layers at each of the three sites

Sites	Depth	Soil type	USDA soil triangle	Bulk density (g/cm^3)	Sand, silt and clay (%)	n	m	η	θ_0	θ_s
126	Surface	Shallow brown earth	Sandy loam	1.17	69, 21, 10	2.36	0.153	8.52	0.41	0.56
	15 cm		Sandy loam	1.09	71, 26, 3	2.40	0.167	7.99	0.37	0.59
	30 cm		Silt loam	1.09	41, 53, 6	2.31	0.134	9.44	0.35	0.59
355	Surface	Brown podzolic	Silt loam	1.02	31, 62, 7	2.28	0.123	10.15	0.34	0.62
	15 cm		Loam	0.90	47, 46, 8	2.32	0.136	9.34	0.15	0.66
	30 cm		Silt loam	0.90	50, 36, 13	2.27	0.118	10.48	0.13	0.66
879	Surface	Sand	Sand	0.79	94, 4, 2	3.03	0.340	4.95	0.18	0.70
	15 cm		Sand	1.29	96, 1, 3	3.38	0.409	4.45	0.13	0.51
	30 cm		Sand	1.29	97, 3, 0	3.39	0.409	4.44	0.13	0.51

n, m and η were estimated using equations (3a), (1b) and (2b), respectively.

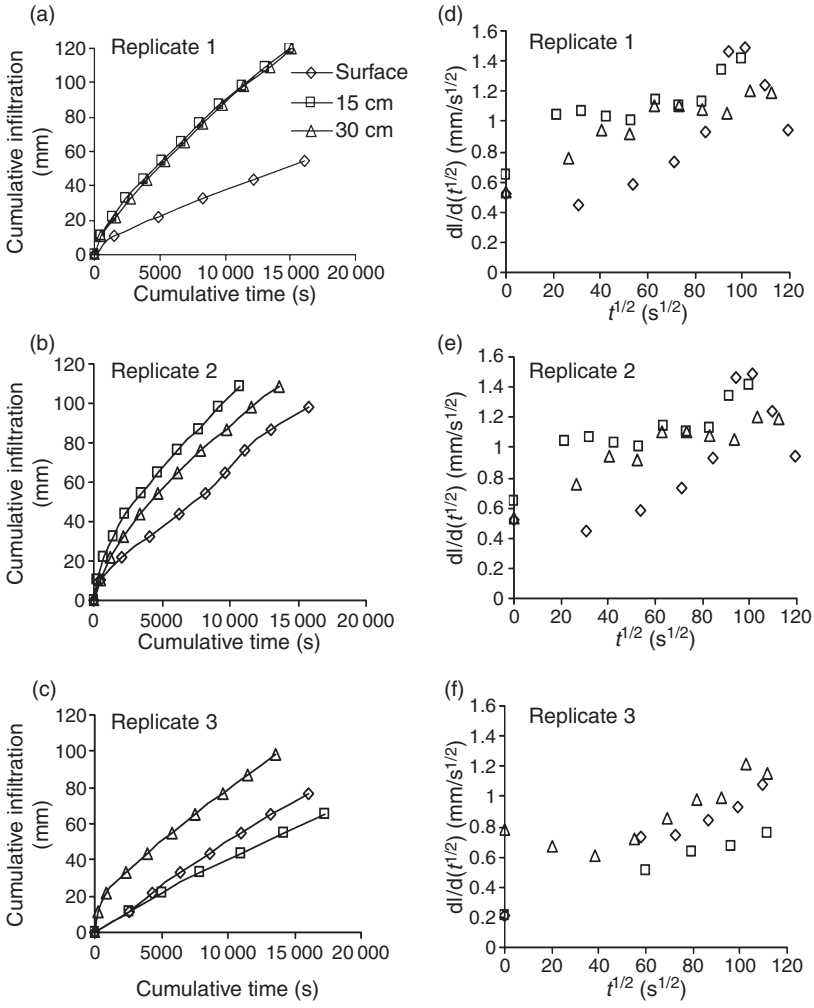

Figure 1 Infiltration for site 126 (shallow brown earth). The points used for DL fitting include all the points of the surface layer, the first three points of the 15-cm layer and the second to fifth points of the 30-cm layer in replicate 1, the second to fourth points of the surface layer, no points for the 15-cm layer and the first three points of the 30-cm layer in replicate 2, the first five points of the surface layer, the first three points of 15-cm layer and the third to sixth points of the 30-cm layer in replicate 3.

With the BEST/I method, S and K_s could not be calculated for replicates 1 and 2 of the surface layer and replicate 3 of the second layer at the shallow brown earth site, and all the replicates of the second and third layers at the sand site (Table 2). This is because infiltration reached steady state early, only a few data points under transient flow state were available for the BEST/I method. For the above locations, this means that the field experiment was conducted during a

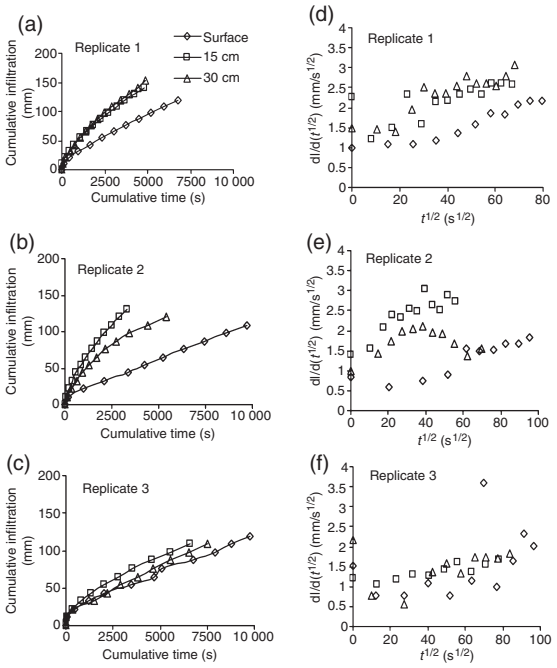

Figure 2 Infiltration for site 355 (brown podzolic). The points used for DL fitting include the third to sixth points of the surface layer, no points of the 15-cm layer and the third to sixth points of the 30-cm layer in replicate 1, the second to fourth points of the surface layer, the second to fourth points of the 15-cm layer and the second to fourth points of the 30-cm layer in replicate 2, no points of the surface layer, the second to fourth points of the 15-cm layer and no points of the 30-cm layer in replicate 3.

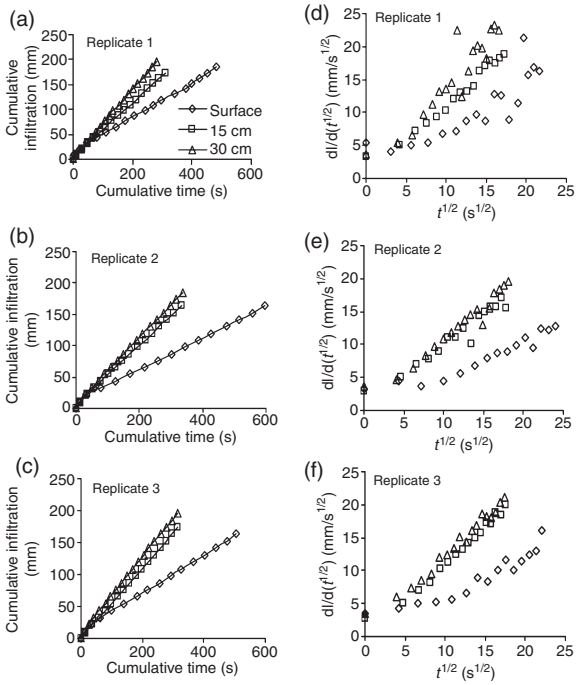

Figure 3 Infiltration for site 879 (sand). The points used for DL fitting include the second to fourth points of the surface layer, the third to sixth points of the 15-cm layer, the first three points of the 30-cm layer in replicate 1, the third to fifth points of the surface layer, the second to fifth points of the 15-cm layer and the second to 11th points of the 30-cm layer in replicate 2, the first three points of the surface layer, the second to fourth points of the 15-cm layer and the second to fifth points of the 30-cm layer in replicate 3.

period when it was not possible to achieve a wide range of soil moisture from the initial to saturated state. For replicate 2 of the second layer at the shallow brown earth site and replicate 2 of the third layer at the brown podzol site, the K_s values are negative and cannot be considered valid. According to equation (4b), K_s can only be negative if $q_s < AS^2$. This usually occurs when S is estimated as a large number. With the DL method, S and K_s could not be calculated for replicate 2 of the second layer at the shallow brown earth site, replicate 2 of the surface layer, replicate 1 of the second layer and replicate 3 of the third layer at the brown podzol site because no clear linear trend could be detected for fitting. For replicates 1 of the surface and second layer, and replicate 2 of the third layer at the shallow brown earth site and replicate 3 of the surface layer at the sand site, the K_s values were negative and could not be considered valid.

A transient flow state is required for the application of both methods. BEST/*I* easily detects whether there is the transient flow state or not. The method does not work if there are too few points under transient flow (Table 2) such that in many cases S and K_s cannot be calculated, especially for the sand site. However, for the DL method, the linear characteristic was evident for all the layers of replicate 1, surface layer of replicate 2 and all the layers of replicate 3 at the shallow brown earth site (Figure 1d–f) and almost all layers of the three replicates at the sand site (Figure 3d–f), although it is clearly under the apparent steady flow state. After further analysis using Equation (8a)

$$\frac{\mathrm{d}I}{\mathrm{d}\sqrt{t}} = \frac{I_{i+1} - I_i}{\sqrt{t_{i+1}} - \sqrt{t_i}} = q(\sqrt{t_{i+1}} + \sqrt{t_i}),$$

we found that $\mathrm{d}I/\mathrm{d}\sqrt{t}$ was actually twice the product of infiltration rate and the square root of time. Therefore, the linear characteristic will be clearer if the infiltration reaches the apparent steady state. If the initial soil moisture is high and approaches saturation very quickly, the DL method is unsuitable as it produces a false result. Similar to the study by Minasny & McBratney (2000), we observed an early time perturbation (Figure 1f, third layer; Figure 2d–f, second layer of replicate 1, surface layer of replicate 2 and all the layers of replicate 3), which was considered as being indicative of the wetting phase of the contact material by Vandervaere *et al.* (2000a). Sorptivity, S, calculated by the two methods appears similar (Table 2), while K_s calculated with DL is one order of magnitude higher than that calculated with the BEST/*I* method. According to Equation (4b),

Table 2 Estimated S and K_s for all replicates of each layer at each site

Sites	Layer	Replicate	h_g (mm)	S (mm/s$^{0.5}$)		K_s (mm/s)		q_s (mm/s)
				BEST	DL	BEST	DL	
126 (shallow brown earth)	Surface	1			0.247		**−0.00544**	0.00277
		2	−4123.1	0.21938	0.231	6.1E−05	0.00217	0.00481
		3			0.24		0.00158	0.00435
	15 cm	1	−284.81	0.33389	0.487	0.00087	**−0.03395**	0.00595
		2	**1421.12**	0.36136		**−0.0003**		0.00721
		3			0.213		0.0016	0.00346
	30 cm	1	−225.37	0.32402	0.21	0.00101	**0.00903**	0.00598
		2	−687.32	0.3603	0.519	0.00034	**−0.01627**	0.00555
		3	−133.78	0.32065	0.267	0.0014	0.00301	0.00554
355 (brown podzolic)	Surface	1	−104.04	0.51489	0.259	0.0042	**0.02185**	0.01406
		2	−52.996	0.37881	0.365	0.00431	**0.10542**	0.00945
		3	−60.548	0.43032		0.00487		0.01164
	15 cm	1	−246.79	0.89019		0.0031		0.01994
		2	−202.21	1.0308	0.807	0.00478	**0.04859**	0.02613
		3	−163.47	0.65171	0.918	0.00236	**−0.02278**	0.01085
	30 cm	1	−133.97	0.92949	0.294	0.00545	**0.06274**	0.02208
		2	**149.719**	0.76614	0.844	**−0.0033**	**0.0141**	0.01109
		3	−48.711	0.5532		0.00521		0.01099
879 (sand)	Surface	1	−37.122	2.6817	3.136	0.23559	**−0.12098**	0.38868
		2	−29.548	2.1662	0.67	0.17485	**0.40443**	0.26510
		3	−28.165	2.4386	3.412	0.22012	**−0.38505**	0.33211
	15 cm	1			1.957		**0.72969**	0.54346
		2			1.301		**0.76225**	0.46441
		3			0.836		**0.90451**	0.55776
	30 cm	1			3.575		0.04863	0.70197
		2			0.22		**1.18091**	0.54346
		3			2.577		0.54723	0.60384

The anomalous values are in bold.

q_s should be greater than K_s, and therefore DL-estimated K_s values were not considered valid because most DL-estimated K_s values were greater than q_s (Table 2).

Hydraulic characteristics of the three soils

Sites 126 (shallow brown earth) and 355 (brown podzolic) have similar soil shape parameters with the highest n and m and the lowest η in the second layer, and the lowest values of n and m and the highest values of η in the third layer. Although the shallow brown earth site has more sand than the brown podzol site, it has lower values of h_g, S and K_s, and higher initial soil water content (Tables 1 and 2). It may be that the soil was more compacted as shown by the higher soil bulk density at the shallow brown earth site than the brown podzol site (Table 1). Compared with the other two sites, the sand site (879) has higher values of n, m and q_s, and lower values of η and initial soil water content because of its very coarse texture (Table 1). Among the three layers at this site, the surface layer has a much lower bulk density than the other two which caused a wider range of soil water content from 0.18 to 0.70. It is also the reason why only the K_s of the surface layer could be calculated with the BEST/I method (enough data points under transient conditions). However, Figure 3a–c clearly demonstrates that the surface layer (with lower bulk density) has a much lower apparent steady infiltration rate than the other two layers (with higher bulk density). It may be that some remnants of grass and moss remained on the soil surface after removal by scissors, and these remnants can delay infiltration and intercept some water.

Analysis of the water retention curves assists in understanding the hydraulic behaviour of the three soils (Lassabatère *et al.*, 2006). We present three groups of water retention and hydraulic conductivity curves (Figure 4a,b), 126a, 879a and others. The surface layer (126a) at the shallow brown earth site was more compacted (higher soil bulk density) which resulted in different water retention and hydraulic conductivity curves than for the others (Figure 4a,b). The surface layer at the sand site (879a) shows a sudden change in water content close to the water pressure step (the air entry potential point) (Figure 4a). Hydraulic conductivity also sharply increases below a given point, and

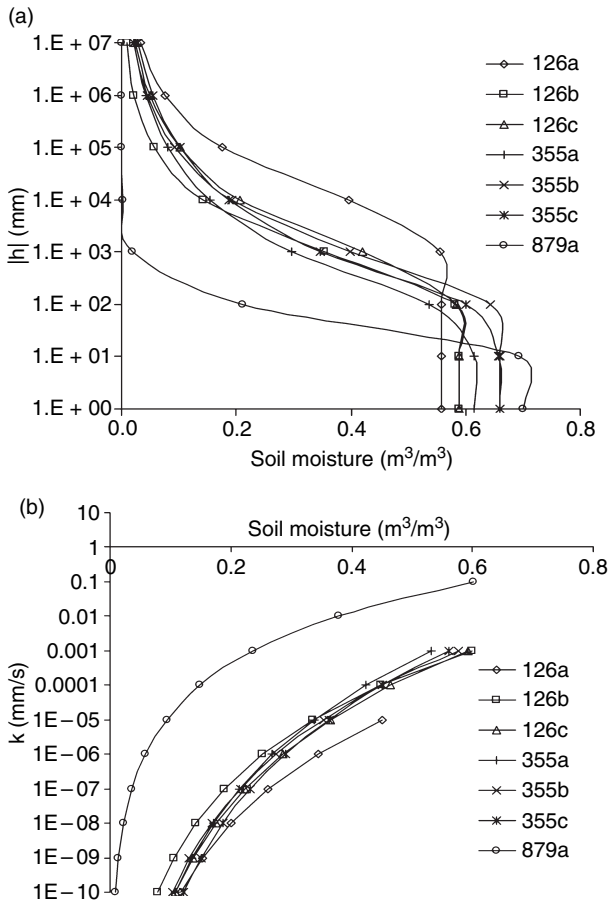

Figure 4 (a) Water retention and (b) hydraulic conductivity curves. (a), (b) and (c) represent the surface, 15- and 30-cm layers, respectively.

then gradually increases beyond that point (Figure 4b). It may be that the particle size distribution of the sand site (at the surface 879a) is close to unimodal (Lassabatère *et al.*, 2006). As a result, most of the pores might saturate when water pressure increases and approaches a pressure step corresponding to the mean pore size. Consequently, both water content and hydraulic conductivity increase considerably. The surface layer at the sand site (879a) is much coarser than the other sites (Table 1) which resulted in saturation at a higher water pressure (Figure 4a) and a higher saturated hydraulic conductivity (Table 2 and Figure 4b).

Conclusion

The DL method did not result in a good estimate of soil hydraulic properties and neither did it identify the transient flow state. The BEST/*I* method is promising. However, the field experiments should have been conducted under a wider range of soil water status from initial to saturated so as to have enough data points under the transient flow state. The dry season is thus recommended for field experiments. There still needs to be more discussion and critical examination of the reasons why for some cases the methods apparently failed to identify K_s and S, also the reasons why negative values were found on occasion. These are important in developing confidence in the method and further research using numerical simulation is needed. Vertical variation in soil hydraulic properties was shown to exist within different layers, especially between the surface and the other two layers. The surface layer had a lower saturated hydraulic conductivity partly caused by compaction (high bulk density) or by remnants of grass. Further research is needed on the effects of compaction and grass on soil hydraulic properties. In this study, contrasting hydraulic behaviour was found between soils of different textures under higher saturated hydraulic conductivity under coarse textures and lesser values with loam textures, especially if compacted.

Acknowledgements

This study was funded by the Irish Environmental Protection Association (EPA) under the Science Technology Research & Innovation for the Environment (STRIVE) Programme 2007–2013 of Ireland (Soil H: Interactions of soil hydrology, land use and climate change and their impact on soil quality; 2007-S-SL-1-S1). We appreciate the discussions with Professor John Albertson of Duke University and Professor Richard Cuenca of Oregon State University. We very much acknowledge the contributions of three anonymous reviewers.

References

Braud, I., De Condappa, D., Sora, J.M., Haverkamp, R., Angulo-Jaramillo, R., Galle, S. & Vauclin, M. 2005. Use of scaled forms of the infiltration equation for the estimation of unsaturated soil hydraulics properties (the Beerkan method). *European Journal of Soil Science*, **56,** 361–374.

Brooks, R.H. & Corey, A.T. 1964. Hydraulic properties of porous media. *Hydrology papers 3*. Colorado State University, Fort Collins, CO.

Burdine, N.T. 1953. Relative permeability calculation from pore size distribution data. *Petroleum Transactions of the American Institute of Mining and Metallurgical Engineering*, **198,** 71–77.

Clapp, R.B. & Hornberger, G.M. 1978. Empirical equations for some soil hydraulic properties. *Water Resources Research*, **14,** 601–604.

van Genuchten, M.T. 1980. A closed-form equation for predicting the hydraulic conductivity of unsaturated soils. *Soil Science Society of America Journal*, **44,** 892–898.

Haverkamp, R., Ross, P.J., Smettem, K.R.J. & Parlange, J.Y. 1994. Three-dimensional analysis of infiltration from disc infiltrometer. 2. Physically based infiltration equation. *Water Resources Research*, **30,** 2931–2935.

Haverkamp, R., Bouraoui, F., Angulo-Jaramillo, R., Zammit, C. & Delleur, J.W. 1998. Soil properties and moisture movement in the unsaturated zone. In: *CRC groundwater engineering handbook* (ed. J.W. Delleur), pp. 5.1–5.50. CRC Press, Boca Raton, FL.

Herbst, M., Diekkruger, B. & Vanderborght, J. 2006. Numerical experiments on the sensitivity of runoff generation to the spatial variation of soil hydraulic properties. *Journal of Hydrology*, **326,** 43–58.

Jacques, D., Mohanty, B.P. & Feyen, J. 2002. Comparison of alternative methods for deriving hydraulic properties and scaling from single-disc tension infiltrometer measurements. *Water Resources Research*, **38,** 25.1–25.14.

Jhorar, R.K., van Dam, J.C., Bastiaanssen, W.G.M. & Feddes, R.A. 2004. Calibration of effective soil hydraulic parameters of heterogeneous soil profiles. *Journal of Hydrology*, **285,** 233–247.

Lassabatère, L., Angulo-Jaramillo, R., Soria Ugalde, J.M., Cuenca, R., Braud, I. & Haverkamp, R. 2006. Beerkan estimation of soil transfer parameters through infiltration experiments – BEST. *Soil Science Society of America Journal*, **70,** 521–532.

Minasny, B. & McBratney, A.B. 2000. Estimation of sorptivity from disc-permeameter measurements. *Geoderma*, **95,** 305–324.

Minasny, B. & McBratney, A.B. 2007. Estimating the water retention shape parameter from sand and clay content. *Soil Science Society of America Journal*, **71,** 1105–1110.

Smettem, K.R.J., Parlange, J.-Y., Ross, J.P. & Haverkamp, R. 1994. Three-dimensional analysis of infiltration from disc infiltrometer. 1. A capillary-based theory. *Water Resources Research*, **30,** 2925–2929.

Vandervaere, J.-P., Vauclin, M. & Elrick, D.E. 2000a. Transient flow from tension infiltrometers. I. The two-parameter equation. *Soil Science Society of America Journal*, **64,** 1263–1272.

Vandervaere, J.-P., Vauclin, M. & Elrick, D.E. 2000b. Transient flow from tension infiltrometers. II. Four methods to determine sorptivity and conductivity. *Soil Science Society of America Journal*, **64,** 1272–1284.